Controlling A-center concentration in silicon through isovalent doping: mass action analysis

S.-R. G. Christopoulos, D. C. Parfitt, E. N. Sgourou, C. A. Londos, R. V. Vovk & A. Chroneos

Journal of Materials Science: Materials in Electronics

ISSN 0957-4522
Volume 27
Number 5

J Mater Sci: Mater Electron (2016) 27:4385-4391
DOI 10.1007/s10854-016-4308-9

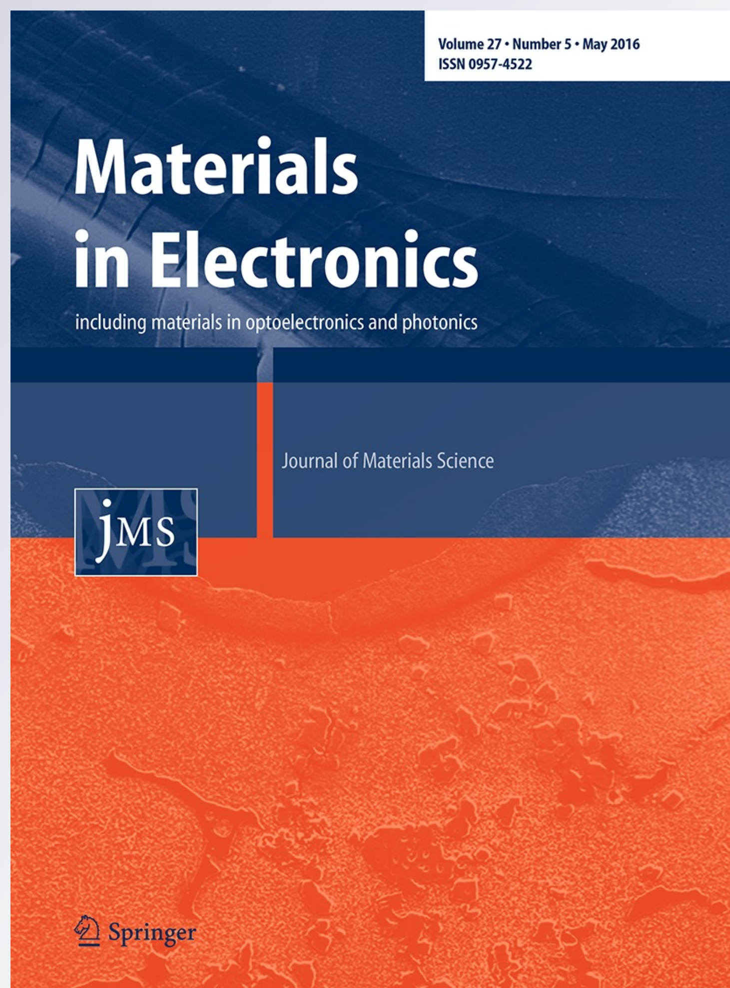

Springer

Your article is protected by copyright and all rights are held exclusively by Springer Science +Business Media New York. This e-offprint is for personal use only and shall not be self-archived in electronic repositories. If you wish to self-archive your article, please use the accepted manuscript version for posting on your own website. You may further deposit the accepted manuscript version in any repository, provided it is only made publicly available 12 months after official publication or later and provided acknowledgement is given to the original source of publication and a link is inserted to the published article on Springer's website. The link must be accompanied by the following text: "The final publication is available at link.springer.com".

Springer

Author's personal copy

J Mater Sci: Mater Electron (2016) 27:4385–4391
DOI 10.1007/s10854-016-4308-9

CrossMark

Controlling A-center concentration in silicon through isovalent doping: mass action analysis

S.-R. G. Christopoulos[1] · D. C. Parfitt[1] · E. N. Sgourou[2] · C. A. Londos[2] · R. V. Vovk[3] · A. Chroneos[1]

Received: 24 November 2015 / Accepted: 2 January 2016 / Published online: 29 January 2016
© Springer Science+Business Media New York 2016

Abstract It has been determined experimentally that doping silicon with large isovalent dopants such as tin can limit the concentration of vacancy-oxygen defects, this in turn, can be deleterious for the materials properties and its application. These results have been supported by recent calculations based on density functional theory employing hybrid functional. In the present study, we employ mass action analysis to calculate the impact of germanium, tin and lead doping on the relative concentrations of vacancy-oxygen defects and defect clusters in silicon under equilibrium conditions. In particular, we calculate how much isovalent doping is required to constrain vacancy-oxygen concentration in silicon and conclude that Sn and Pb doping are the most effective isovalent dopants. The results are discussed in view of recent experimental and computational results.

1 Introduction

Silicon (Si) is the semiconductor material with the largest number of applications in microelectronic, sensor and photovoltaic devices. As a result, it is one of the most studied and understood systems; despite this, the understanding of many defect processes that affect its properties are still lacking [1–4]. These defect processes are, however, becoming progressively more important as devices are miniaturized and the overall dimensions of the optically or electronically active part are reduced.

The *VO* or A-center is the most important and studied oxygen-vacancy defect in Czochralski grown Si (Cz-Si) [5]. A-centers form by the trapping of a relatively high concentration of oxygen during the Czochralski crystal growth process [5]. A-centers form by the association of oxygen interstitials (O_i) with vacancies (*V*) via the reaction $V + O_i \rightarrow VO$ [5–7]. The presence of A-centers can impact device performance as they are electrically and optically active. An example of the importance of A-centers is Si-based imaging and spectroscopy sensors in space. Space is a radiation environment and the formation of A-centers is significant as high-energy particles induce lattice displacement damage resulting in a highly athermal concentration of *V*. These in turn diffuse and bind with oxygen atoms. These A-centers are deemed to be effective traps that have a detrimental impact upon device performance [8, 9]. Therefore it is necessary to suppress their concentration and for this purpose numerous defect engineering strategies have been proposed.

Carbon (C) is a common impurity being introduced in the Si lattice during the crystal growth process from the graphitic components in the equipment, gaseous contaminants and the polycrystalline starting material [10–12]. C may occupy substitutional sites (C_s) forming charge neutral defects in the Si lattice. C atoms can also associate with O_i to form C–O complexes, such as C_s–O_i pairs [13]. An important process in irradiated Si is the Watkins displacement reaction $C_s + Si_I \rightarrow C_i$ that can lead to the formation of C interstitials (C_i) and the suppression of Si intertitials (Si_I) [14, 15]. Importantly, it was previously shown that C_i introduces in-gap states [16], whereas at

✉ A. Chroneos
ab8104@coventry.ac.uk

[1] Faculty of Engineering, Environment and Computing, Coventry University, Priory Street, Coventry CV1 5FB, UK

[2] Solid State Physics Section, University of Athens, Panepistimiopolis Zografos, 157 84 Athens, Greece

[3] Physics Department, V. Karazin Kharkiv National University, Svobody Sq. 4, Kharkiv 61077, Ukraine

Author's personal copy

room temperature it associates with O_i and C_s forming C_iO_i and C_iC_s defects [17–19]. These defects in turn introduce states within the Si band gap, which can impact devices [20–22] and therefore their structure and properties have been thoroughly investigated [23–27]. Finally, during irradiation C_i, C_iO_i, and C_iC_s defects are nucleation centres for more extended defects such as $C_iO_iSi_I$ [28–30].

The experimental studies of Watkins [31, 32] and Kimerling et al. [33]. demonstrated that isovalent impurities [carbon (C), germanium (Ge) and tin (Sn)] can impact the formation processes of *V*O pairs in Si. In more recent studies, the trend has been to introduce Sn in Si (and/or related host materials such as Ge) at ever increasing concentrations as this leads to the variation of the structural and electronic properties [34–36]. From an experimental viewpoint, electron irradiation experiments determined that the precense of dopant Sn atoms suppresses the formation of the A-centers [37]. Additionally, Pb causes [38] a reduction in the *V*O concentration, which is larger in comparison with that caused by Sn [39]. The decrease of the *V*O concentration has been attributed [39–41] to the reduced recombination of Frenkel pairs during irradiation due to the oversized isovalent dopants. These earlier results have been recently supported by recent work employing infrared spectroscopy and density functional theory (DFT) calculations [40, 41]. Mass action analysis can clarify and deconvolute the role of doping on dopant-defect interactions and in particular which interactions will lead to significant concentration of defects [42].

The aim of the present study is to employ mass action analysis to calculate the impact of isovalent dopants upon the relative concentrations of oxygen-vacancy defects and in particular *V*O.

2 Methodology

2.1 Definitions

Defect clusters compete for point defects, and therefore to establish the overall defect populations, it is required to consider the formation of all defects types (isolated point defects and clusters) and to calculate their relative populations through a mass action analysis [43]. DFT calculations can be used in conjunction with experimental work to provide estimates of the relative thermal stability and formation energy of defect clusters. In that respect the calculation of the binding energies, E_b, defined by the following relation is important:

$$E_b = E_{\text{defect cluster}} - \Sigma E_{\text{isolated defects}} \quad (1)$$

Equation 1 implies that for negative binding energies clusters are energetically favourable with respect to their constituent isolated defect components. In the present study we use recent state-of-the-art hybrid DFT binding energies calculated by Wang et al. [44–46].

2.2 Mass action analysis

The concentration of an *XY* defect cluster (denoted by [*XY*]) with a binding energy E_b relative to the concentration of unbound defects X and Y (i.e. [*X*] and [*Y*] respectively) is defined by:

$$\frac{[XY]}{[X][Y]} = \exp\left(\frac{-E_b}{k_B T}\right) \quad (2)$$

where k_B is Boltzmann's constant and T is the temperature.

The mass action method was previously employed to calculate the relative concentrations of point defects and their clusters in germanium (Ge) [47, 48] and Si [49]. It should be stressed that within the mass action framework the temperature dependence of defect concentrations at equilibrium conditions may be calculated. Kinetics may impact the results as will non-equilibrium conditions (for example high dose rate irradiation). In the present study the relative concentrations of the defects are predicted under equilibrium conditions.

3 Results and discussion

3.1 Mass action model

Experimental FTIR spectroscopy studies have determined that the main defect clusters in irradiated Si are *V*O, V_2, VO_2, C_i, C_iO_i, C_iC_s, and $C_iO_iSi_I$ [50]. Additionally, there is experimental and/or theoretical evidence of the *DV* and *DV*O defects in isovalent (*D*)-doped Si (*D* = Pb, Sn, Ge) [39–41, 46, 47, 51]. The respective relations for the formation of the defects are:

$$V + O \rightarrow VO \quad (3)$$

$$V + V \rightarrow VV \quad (4)$$

$$VO + O_i \rightarrow VO_2 \quad (5)$$

$$C_s + Si_I \rightarrow C_i \quad (6)$$

$$C_i + O_i \rightarrow C_iO_i \quad (7)$$

$$C_i + C_s \rightarrow C_iC_s \quad (8)$$

$$C_iO_i + Si_I \rightarrow C_iO_iSi_I \quad (9)$$

$$D + V \rightarrow DV \quad (10)$$

$$D + V + O_i \rightarrow DVO \quad (11)$$

Author's personal copy

Previous studies [50] have shown that the interaction between isovalent dopants and C atoms is limited at least as compared to binding energies of the *DV* and *DV*O defects. Additionally, in a previous mass action analysis study it was calculated that a typical C-concentration has limited impact upon the formation of *V*O defects [52]. Finally, the main aim of the present study is to deconvolute and assess the impact of isovalent doping on the relative concentrations of oxygen-vacancy defects and in particular *V*O. Therefore, we omit from the mass action model the C-related reactions (i.e. Eqs. 6–9).

The system (i.e. Eqs. 3–5, 10, 11) can be described using mass action by solving simultaneously the following relations:

$$\frac{[VV]}{[V][V]} = \exp\left(\frac{2.52\ \text{eV}}{k_B T}\right) \qquad (12)$$

$$\frac{[VO_i]}{[V][O_i]} = \exp\left(\frac{2.21\ \text{eV}}{k_B T}\right) \qquad (13)$$

$$\frac{[VO_2]}{[V][O_i][O_i]} = \exp\left(\frac{4.05\ \text{eV}}{k_B T}\right) \qquad (14)$$

$$\frac{[DV]}{[D][V]} = \exp\left(\frac{-E_b(DV)}{k_B T}\right) \qquad (15)$$

$$\frac{[DVO_i]}{[D][V][O_i]} = \exp\left(\frac{-E_b(DVO_i)}{k_B T}\right) \qquad (16)$$

For the binding energies in Eqs. 12–16 the hybrid DFT values derived by Wang et al. [44–46]. were used. In the present study we consider concentrations of Si_I and *V* significantly higher than the thermal equilibrium concentration. This is because under irradiation there is the formation of a highly athermal concentration of Si_I and *V*. These native point defects interact with oxygen and carbon forming the complexes mentioned above.

3.2 Impact of isovalent doping

Ge is the smallest isovalent dopant considered here. Ge*V* and Ge*V*O have binding energies of −0.26 and −2.44 eV respectively [46]. Figure 1(a) represents the temperature dependence of the concentration of unbound atoms and defect clusters for initially unbound [Ge] = 10^{17} cm^{-3} and $[O_i] = [V] = [Si_I] = 10^{18}$ cm^{-3} over the temperature range 400–1600 K. For this low Ge content, the most populous defects are the VO_2 and V_2. Ge*V*O entraps a small concentration of *V* and O_i peaking to 1 % at the highest temperatures considered. The Ge*V* defects have very small concentrations throughout the *T* range. For initially

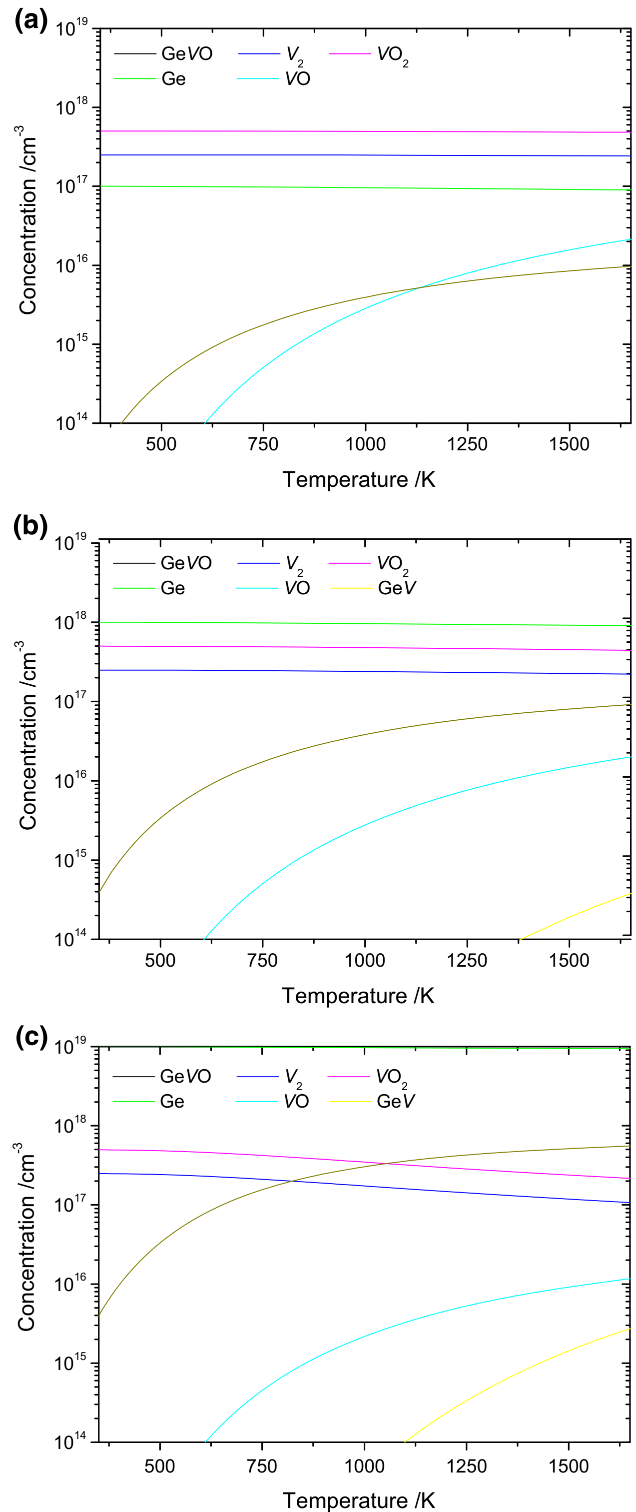

Fig. 1 The temperature dependence of unbound atoms and defect clusters for $[O_i] = 1 \times 10^{18}$ cm^{-3}, initial $[V] \equiv [Si_I] = 1 \times 10^{18}$ cm^{-3} and **a** [Ge] = 1×10^{17} cm^{-3}, **b** [Ge] = 1×10^{18} cm^{-3}, and **c** [Ge] = 1×10^{19} cm^{-3}

Author's personal copy

unbound [Ge] = 10^{18} cm^{-3} (refer to Fig. 1b) the VO_2 and V_2 defects remain the most populous, there is a considerable increase of the GeVO defects, however, the concentration of VO defects is similar to the case with less Ge doping. The GeV defects are increased but they are still less than 10^{14} cm^{-3} for most of the T considered. Interestingly, at the higher Ge concentration (for initially unbound [Ge] = 10^{19} cm^{-3}) at around T = 1000 K the GeVO becomes the dominant vacancy-complex exceeding the concentration of both the VO_2 and V_2 defects (refer to Fig. 1c). The GeV content, as expected, significantly increases as compared to the lower Ge-concentration cases but is far less populous as compared to GeVO. VO is decreased but not significantly to justify the use of Ge doping as a strategy to reduce its concentration.

Sn is larger than Ge and this is reflected in its higher vacancy complex binding energies, which are for SnV and SnVO −1.50 and −3.19 eV respectively [46]. Figure 2a represents the temperature dependence of the concentration of unbound atoms and defect clusters for initially unbound [Sn] = 10^{17} cm^{-3} and $[O_i] = [V] = [Si_I] = 10^{18}$ cm^{-3} over the temperature range 400–1600 K. Again the VO_2 and V_2 defects are the most populous followed by SnVO, where most of the Sn atoms are clustered (refer to Fig. 2a). The SnV defect acquires significant concentration as the temperature increases accounting for about 10 % of the Sn atoms and 1 % of the V at temperatures greater than 1500 K (refer to Fig. 2a). An order of magnitude increase in the Sn concentration (Fig. 2b) leads to the significant decrease of the VO_2 and V_2. Additionally, SnV has now a similar concentration to VO_2, and the population of VO is significantly reduced. As the temperature increases SnV captures nearly 10 % of the Sn and V species. A further increase of the Sn concentration by an order of magnitude leads to thedominance of the SnVO and SnV defects (refer to Fig. 3c). Most V are tapped by SnVO and this leads to the collapse of the VO concentration to below 10^{14} cm^{-3} i.e. to a reduction of more than two orders of magnitude throughout the T range considered.

Pb is more bound to V and VO than Ge and this is reflected in its higher binding energies, which are for PbV and PbVO −1.80 and −3.47 eV respectively [46]. As the binding energy difference between Sn-vacancy complexes and Pb-vacancy complexes are not very high the impact of Pb defect on the oxygen-related defects in Si is similar.

To clarify the effect of Sn and Pb concentration at reducing VO concentration we introduce Fig. 4, where its concentration with respect to D for four typical temperatures is considered. For all the temperatures considered VO is reduced efficiently when the Sn and Pb doping is more than 10^{18} cm^{-3}. There is little if any difference (Pb being slightly better) between Sn and Pb in their suppression of VO defects. This is consistent with the small amount of available experimental evidence (Ref. 50 and references therein) and is a reflection of the higher binding energies of Sn and Pb related defects as compared to Ge related defects.

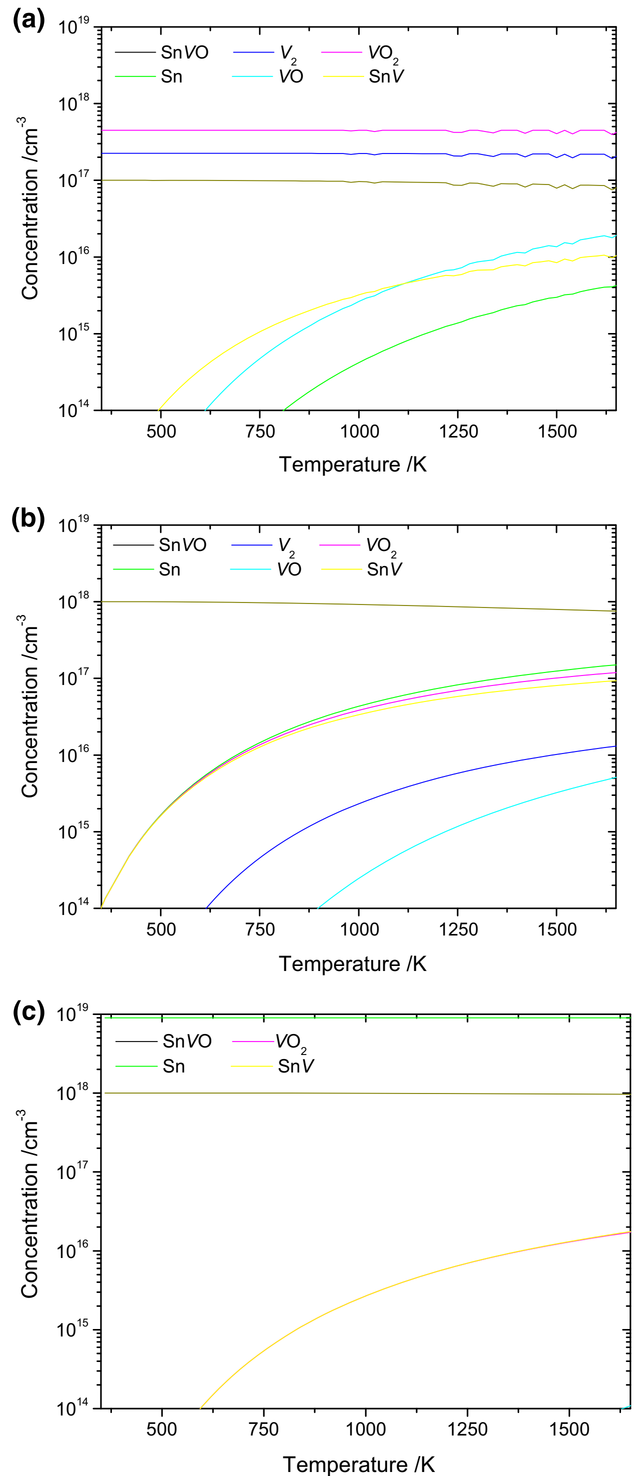

Fig. 2 The temperature dependence of unbound atoms and defect clusters for $[O_i] = 1 \times 10^{18}$ cm^{-3}, initial $[V] \equiv [Si_I] = 1 \times 10^{18}$ cm^{-3} and **a** [Sn] = 1×10^{17} cm^{-3}, **b** [Sn] = 1×10^{18} cm^{-3}, and **c** [Sn] = 1×10^{19} cm^{-3}

Author's personal copy

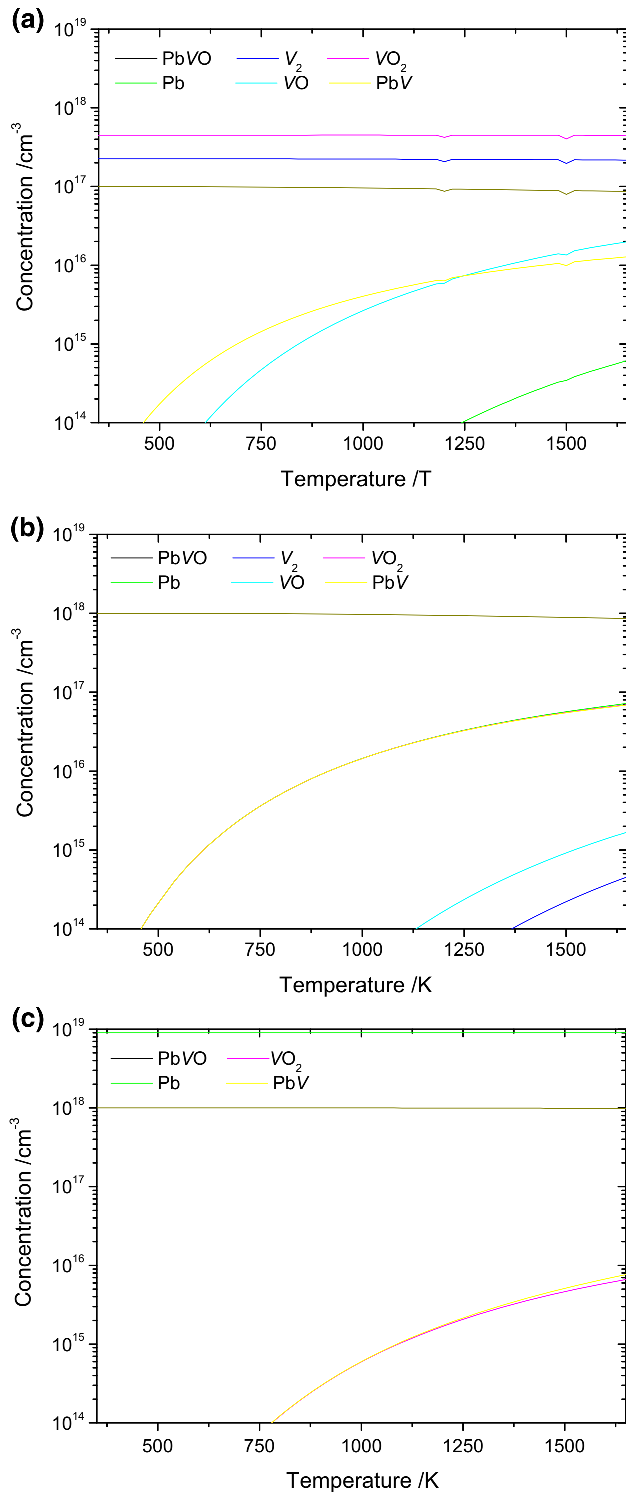

Fig. 3 The temperature dependence of unbound atoms and defect clusters for $[O_i] = 1 \times 10^{18}$ cm^{-3}, initial $[V] \equiv [Si_I] = 1 \times 10^{18}$ cm^{-3} and **a** $[Pb] = 1 \times 10^{17}$ cm^{-3}, **b** $[Pb] = 1 \times 10^{18}$ cm^{-3}, and **c** $[Pb] = 1 \times 10^{19}$ cm^{-3}

At this point we should consider that Pb is co-doped with C in order to be introduced in Si. In essence the presence of C with its smaller covalent radius relieves the strains introduced by Pb atoms that are significantly larger compared to Si atoms. In the case of Pb doping C is important to retain Pb atoms at their sites and to avoid Pb precipitation, which is a significant issue [38, 53, 54]. Nevertheless, introducing further C in the lattice can lead to more C-related defects that can be in turn deleterious for the properties of Si [50, 55]. Conversely, Sn doping at around 10^{18} cm^{-3} does not require codoping with C and therefore given its similar efficiency with Pb at reducing *VO* defects it is a better choice.

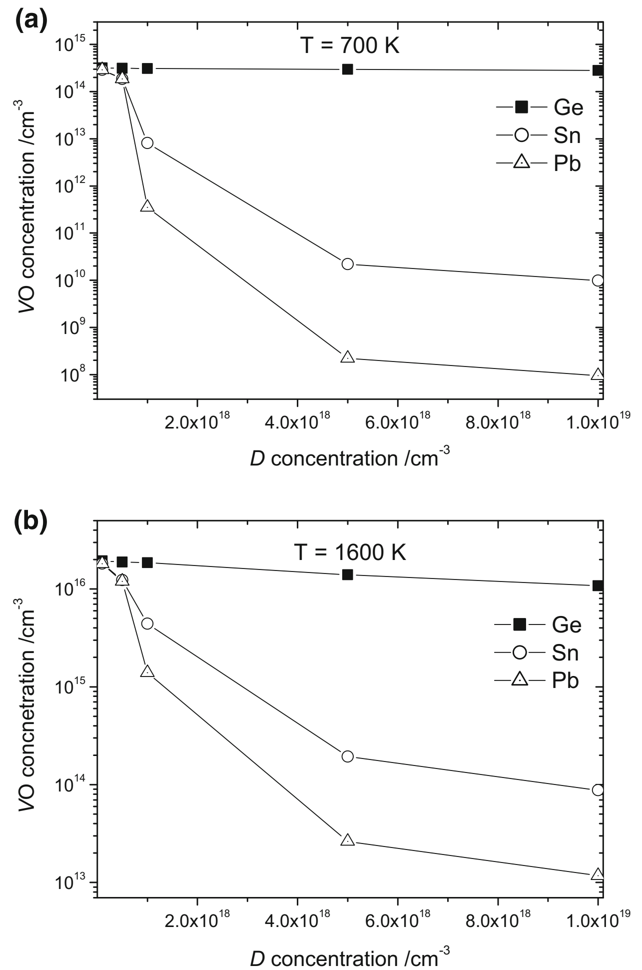

Fig. 4 The concentration of *VO* with respect to *D* for **a** T = 700 K and **b** T = 1600 K

Importantly, the aim of the present study is the calculation of relative defect concentrations at equilibrium conditions aiming to show the influence of different isovalent dopants. These form defect clusters with *V* and O_i taking into advantage predominately the local strain relaxation as reflected by their binding energies of the clusters (refer to Eq. 1). Kinetics and/or extended defects always play a role in defect processes and particularly in experiments which involve irradiation and are under non-equilibrium conditions.

Author's personal copy

The predicted formation of *V*O defects at high temperature may not be compatible with irradiation experiments where they have transformed to VO_n defects. The mass action results are consistent with crystal growth experiments as in these there is evidence that *V*O defects form at high temperature [52]. Binding energies alone are not sufficient to predict the thermal evolution of the system as demonstrated during annealing of irradiated Si, however, they are important when comparing the efficacy of isovalent dopants and the relative concentrations required to reduce the deleterious *V*O defects. Finally, the inclusion of the isovalent dopant may impact other defect processes and electronic properties in Si as it impacts other group IV materials [56–58]

4 Conclusions

In the present study a mass action analysis model was employed to deconvolute the impact of isovalent doping on oxygen related defects in Si. The mass action analysis model uses hybrid DFT derived binding energies of the releavant clusters and concerns equilibrium conditions. The relative concentration of defects are predicted under an extensive temperature range for different Ge, Sn and Pb concentration conditions. It is shown here that Sn and Pb doping (exceeding 10^{18} cm^{-3}) more efficiently suppresses *V*O. Considering the techological issues to introduce high concentrations of Pb in Si it is deemed that Sn is a more appropriate isovalent dopant to reduce the concentration of oxygen-related defects in Si.

Acknowledgments SRGC and AC are grateful for funding from the Lloyd's Register Foundation, a charitable foundation helping to protect life and property by supporting engineering-related education, public engagement and the application of research.

References

1. V.V. Emtsev, N.V. Abrosimov, V.V. Kozlovskii, G. Oganesyan, Semiconductors **48**, 1438 (2014)
2. L.I. Murin, J.L. Lindstrom, B.G. Svensson, V.P. Markevich, A.R. Peaker, C.A. Londos, Solid State Phenom. **108–109**, 267 (2005)
3. H. Bracht, A. Chroneos, J. Appl. Phys. **104**, 076108 (2008)
4. C. Gao, X. Ma, J. Zhao, D. Yang, J. Appl. Phys. **113**, 093511 (2013)
5. R.C. Newman, R. Jones, "Oxygen in silicon" in *Semiconductors and Semimetals*, ed. by F. Shimura (Academic Press, Orlando, 1994), vol 42, p. 289
6. J.W. Corbett, G.D. Watkins, R.S. McDonald, Phys. Rev. A **135**, 1381 (1964)
7. C.A. Londos, Phys. Stat. Sol. A **102**, 639 (1987)
8. C.A. Londos, E.N. Sgourou, D. Hall, A. Chroneos, J. Mater. Sci.: Mater. Electron. **25**, 2395 (2014)
9. D.J. Hall, N.J. Murray, J.P.D. Gow, D. Wood, A. Holland, J. Instrum. **9**, C12004 (2014)
10. B.O. Kolbersen, A. Muhlbauer, Solid State Electron. **25**, 759 (1982)
11. R.C. Newman, Mater. Res. Soc. Symp. Proc. **59**, 403 (1986)
12. W. Scorupa, R.A. Yankov, Mater. Chem. Phys. **44**, 101 (1996)
13. G. Davies, E.C. Lightowlers, R.C. Newman, A.S. Oates, Semicond. Sci. Technol. **2**, 524 (1987)
14. R.C. Newman, A.R. Bean, Radiat. Eff. **8**, 189 (1970)
15. G.D. Watkins, K.L. Brower, Phys. Rev. Lett. **36**, 1329 (1976)
16. C.A. Londos, Phys. Rev. B **35**, 6295 (1987)
17. E.V. Lavrov, L. Hoffmann, B.B. Nielsen, Phys. Rev. B **60**, 8081 (1999)
18. C.A. Londos, M.S. Potsidi, E. Stakakis, Phys. B **340–342**, 551 (2003)
19. C.-L. Liu, W. Windl, L. Borucki, S. Lu, X.-Y. Liu, Appl. Phys. Lett. **80**, 52 (2002)
20. G. Davies, R.C. Newman, in *Handbook of Semiconductors*, ed. by S. Mahajan (Elsevier, Amsterdam, 1994), vol 3, p. 1557
21. M. Yamaguchi, A. Khan, S.J. Taylor, K. Ando, T. Yamaguchi, S. Matsuda, T. Aburaya, J. Appl. Phys. **86**, 217 (1999)
22. K. Murata, Y. Yasutake, K. Nittoh, S. Fukatsu, K. Miki, AIP Adv. **1**, 032125 (2011)
23. J.M. Trombetta, G.D. Watkins, Appl. Phys. Lett. **51**, 1103 (1987)
24. R. Jones, S. Oberg, Phys. Rev. Lett. **68**, 86 (1991)
25. J. Coutinho, R. Jones, P.R. Briddon, S. Oberg, L.I. Murin, V.P. Markevich, J.L. Lindstrom, Phys. Rev. B **65**, 014109 (2001)
26. P. Leery, R. Jones, S. Oberg, V.J.B. Torres, Phys. Rev. B **55**, 2188 (1997)
27. R.B. Capaz, A. Dal Pino Jr, J.D. Joannopoulos, Phys. Rev. B **58**, 9845 (1998)
28. A. Mattoni, F. Bernantini, L. Colombo, Phys. Rev. B **66**, 195214 (2002)
29. C.A. Londos, M.S. Potsidi, G.D. Antonaras, A. Andrianakis, Phys. B **376–377**, 165 (2006)
30. D.J. Backlund, S.K. Estreicher, Phys. Rev. B **77**, 205205 (2008)
31. G.D. Watkins, I.E.E.E. Trans, Nucl. Sci. **16**, 13 (1969)
32. G.D. Watkins, Phys. Rev. B **12**, 4383 (1975)
33. L.C. Kimerling, M.T. Asom, J.L. Benton, P.J. Drevinsky, C.E. Caefer, Mater. Sci. Forum **38–41**, 141 (1989)
34. A. Chroneos, C. Jiang, R.W. Grimes, U. Schwingenschlogl, H. Bracht, Appl. Phys. Lett. **95**, 112101 (2009)
35. S. Takeuchi, Y. Shimura, O. Nakatsuka, S. Zaima, M. Ogawa, A. Sakai, Appl. Phys. Lett. **92**, 231916 (2008)
36. A. Chroneos, C. Jiang, R.W. Grimes, U. Schwingenschlögl, H. Bracht, Appl. Phys. Lett. **94**, 252104 (2009)
37. C. Claeys, E. Simoen, V.B. Neimash, A. Kraitchinskii, M. Kras'ko, O. Puzenko, A. Blondeel, P. Clauws, J. Electrochem. Soc. **146**, G738 (2001)
38. M.L. David, E. Simoen, C. Claeys, V. Neimash, M. Kras'ko, A. Kraitchinskii, V. Voytovych, A. Kabaldin, J.F. Barbot, Solid State Phenom. **108–109**, 373 (2005)
39. C.A. Londos, D. Aliprantis, E.N. Sgourou, A. Chroneos, P. Pochet, J. Appl. Phys. **111**, 123508 (2012)
40. A. Chroneos, C.A. Londos, E.N. Sgourou, P. Pochet, Appl. Phys. Lett. **99**, 241901 (2011)
41. E.N. Sgourou, D. Timerkaeva, C.A. Londos, D. Aliprantis, A. Chroneos, D. Caliste, P. Pochet, J. Appl. Phys. **113**, 113506 (2013)
42. A. Chroneos, H. Bracht, R.W. Grimes, B.P. Uberuaga, Mater. Sci. Eng. B **154–155**, 72 (2008)
43. F.A. Kröger, V.J. Vink, in *Solid State Physics*, ed. by F. Seitz and D. Turnbull (Academic, New York, 1956), vol 3, p. 307
44. H. Wang, A. Chroneos, C.A. Londos, E.N. Sgourou, U. Schwingenschlögl, Appl. Phys. Lett. **103**, 052101 (2013)
45. H. Wang, A. Chroneos, C.A. Londos, E.N. Sgourou, U. Schwingenschlögl, Sci. Rep. **4**, 4909 (2014)
46. H. Wang, A. Chroneos, C.A. Londos, E.N. Sgourou, U. Schwingenschlögl, Phys. Chem. Chem. Phys. **16**, 8487 (2014)

Author's personal copy

47. A. Chroneos, R.W. Grimes, B.P. Uberuaga, S. Brotzmann, H. Bracht, Appl. Phys. Lett. **91**, 192106 (2007)
48. G. Impellizzeri, S. Boninelli, F. Priolo, E. Napolitani, C. Spinella, A. Chroneos, H. Bracht, J. Appl. Phys. **109**, 113527 (2011)
49. M.J. Powell, S.C. Deane, Phys. Rev. B **53**, 10121 (1995)
50. A. Chroneos, E.N. Sgourou, C.A. Londos, U. Schwingenschlögl, Appl. Phys. Rev. **2**, 021306 (2015)
51. A. Chroneos, C.A. Londos, E.N. Sgourou, J. Appl. Phys. **110**, 093507 (2011)
52. V.V. Voronkov, R. Falster, J. Electrochem. Soc. **149**, G167 (2002)
53. V.B. Neimash, V.V. Voitovych, A.M. Kraitchinskii, L.I. Shpinar, M.M. Krasko, V.M. Popov, A.P. Pokanevych, M.I. Gorodyskyi, Y.V. Pavlovskyi, V.M. Tsmots, O.M. Kabaldin, Ukr. J. Phys. **50**, 492 (2005)
54. K. Milants, J. Verheyden, T. Balancira, W. Deweerd, H. Pattyn, S. Bukshpan, D.L. Williamson, F. Vermeiren, G. Van Tendeloo, C. Viekken, S. Libbrecht, C. Van Haesendonck, J. Appl. Phys. **81**, 2148 (1997)
55. A. Chroneos, C.A. Londos, J. Appl. Phys. **107**, 093518 (2010)
56. A. Chroneos, R.W. Grimes, H. Bracht, J. Appl. Phys. **105**, 016102 (2009)
57. A. Chroneos, H. Bracht, Appl. Phys. Rev. **1**, 011301 (2010)
58. A. Chroneos, J. Appl. Phys. **107**, 076102 (2010)